Published in final edited form as:
Circ Res. 2011 April 1; 108(7): 847–856. doi:10.1161/CIRCRESAHA.111.240234.

Dynamic Calcium Movement inside Cardiac Sarcoplasmic Reticulum during Release

Eckard Picht[1], **Aleksey V. Zima**[3], **Thomas R. Shannon**[2], **Alexis M. Duncan**[3], **Lothar A. Blatter**[2], and **Donald M. Bers**[1,3]

[1]Department of Pharmacology, University of California, Davis, Davis, CA 95616, USA

[2]Department of Molecular Biophysics and Physiology, Rush University, Chicago, IL 60612

[3]Department of Cell and Molecular Physiology, Loyola University, Chicago Maywood, IL 60153

Abstract

Rationale—Intra-sarcoplasmic reticulum (SR) free [Ca] ($[Ca]_{SR}$) provides the driving force for SR Ca release and is a key regulator of SR Ca release channel gating during normal SR Ca release or arrhythmogenic spontaneous Ca release events. However, little is known about $[Ca]_{SR}$ spatiotemporal dynamics.

Objective—To directly measure local $[Ca]_{SR}$ with subsarcomeric spatiotemporal resolution during both normal global SR Ca release and spontaneous Ca sparks, and to evaluate the quantitative implications of spatial $[Ca]_{SR}$ gradients.

Methods & Results—Intact and permeabilized rabbit ventricular myocytes were subjected to direct simultaneous measurement of cytosolic [Ca] and $[Ca]_{SR}$ and fluorescence recovery after photobleach (FRAP). We found no detectable $[Ca]_{SR}$ gradients between SR release sites (junctional SR) and Ca uptake sites (free SR) during normal global Ca release, clear spatio-temporal $[Ca]_{SR}$ gradients during isolated Ca blinks, faster intra-SR diffusion in the longitudinal vs. transverse direction, 3-4 fold slower diffusion of fluorophores in the SR than in cytosol, and that intra-SR Ca diffusion varies locally, dependent on local SR connectivity. A computational model clarified why spatiotemporal gradients are more detectable in isolated local releases vs. global releases and provides a quantitative framework for understanding intra-SR Ca diffusion.

Conclusions—Intra-SR Ca diffusion is rapid, limiting spatial $[Ca]_{SR}$ gradients during excitation-contraction coupling. Spatiotemporal $[Ca]_{SR}$ gradients are apparent during Ca sparks, and these observations constrain models of dynamic Ca movement inside the SR. This has important implications for myocyte SR Ca handling, synchrony and potentially arrhythmogenic spontaneous contraction.

Corresponding Author: Donald M. Bers, PhD, Department of Pharmacology, Genome Building 6513, University of California, Davis, 451 Health Sciences Drive, Davis, CA 95616 USA, Tel: 530-752-6517, Fax: 530-752-7710, dmbers@ucdavis.edu .

Disclosures
None.

Subject codes: [132], [152]

Keywords

cardiac excitation-contraction coupling; sarcoplasmic reticulum; Ca sparks; Ca transport; ryanodine receptor

INTRODUCTION

The sarcoplasmic reticulum (SR) is the main Ca storage organelle in cardiac myocytes. SR Ca release during excitation-contraction coupling (ECC) contributes the majority of Ca for cytosolic Ca transients and contractile activation.[1,2] SR Ca load critically regulates SR Ca release during both ECC and spontaneous SR Ca release,[3-5] which can cause delayed afterdepolarizations and arrhythmias. Local SR Ca depletion is believed to play a role in terminating SR Ca release[6] and contribute to defective Ca handling in myocytes during heart failure and arrhythmias.

Local intra-SR Ca has important functional implications for control of physiological and pathophysiological SR Ca release. Slow intra-SR Ca diffusion would promote non-uniform distribution of SR Ca load and intra-SR free [Ca] ($[Ca]_{SR}$) within the network. This could induce regions that are more likely to release Ca spontaneously or upon a Ca trigger (in regions with higher $[Ca]_{SR}$) vs. regions that are less likely to release Ca (with lower local $[Ca]_{SR}$). Fast intra-SR Ca diffusion on the other hand, would tend to level intra-SR Ca gradients and contribute to an even supply of Ca to SR Ca release sites throughout the cardiac myocyte. Furthermore, this would limit local delays in intra-SR Ca movement from Ca uptake to Ca release sites within the SR, that could otherwise contribute to reduced SR Ca availability at short diastolic intervals and hence the induction and maintenance of cardiac alternans.

Electron microscopic studies show that the SR is a continuous network with sporadic connections across and along Z-lines.[7-9] Wu & Bers[10] provided direct functional evidence for continuity of the entire SR and nuclear envelope lumens in adult rabbit cardiac myocytes, using fluorescence recovery after photobleach (FRAP) of an intra-SR Ca indicator (Fluo-5N)[11] and Ca movement throughout the SR network. They estimated relatively fast diffusion coefficients for Fluo-5N and Ca within the SR (~10 times slower than free diffusion in solution). Another study confirmed the functional SR continuity (using indirect methods), but estimated a 7-fold lower intra-SR Ca diffusion coefficient[12] than ours.[10] Moreover, their computer model suggested that SR Ca release at one junctional SR (JSR) would cause little depletion in neighboring free SR (FSR). Here we sought to measure spatiotemporal features of FSR vs. JSR depletion during local Ca release and assess intra-SR diffusion using local FRAP.

This study was designed to test: 1) whether appreciable JSR-FSR $[Ca]_{SR}$ gradients occur during ECC or local SR Ca release events, 2) whether intra-SR Ca diffusion on a sarcomeric scale occurs preferentially in longitudinally vs. transversally, and 3) examine how spatiotemporal gradients constrain quantitative understanding of SR Ca handling.

METHODS

An Online Supplement contains methodological details. Rabbit ventricular myocytes were isolated, loaded with cell-permeant low affinity Ca indicator Fluo-5N (K_d ~400 μM/L) to measure $[Ca]_{SR}$ via confocal microscopy combined with $[Ca]_i$ measurements using Rhod-2.[6,11,13,14] Standard intact myocyte superfusate (2 mmol/L $CaCl_2$) and saponin-permeabilized myocyte solutions (150 nM free $[Ca]_i$) were used at 21-24°C. Cytosolic and

intra-SR FRAP used Calcein/AM and Fluo-5N/AM loaded cardiomyocytes, respectively. Data are mean ±SEM with statistical significance (P<0.05) determined by Student's *t* test.

RESULTS

Limited $[Ca]_{SR}$ spatial gradients accompany ECC

To test for detectable intra-SR free Ca ($[Ca]_{SR}$) gradients between Ca release sites (JSR) and non-junctional free SR sites (FSR) during Ca transients, we used spatially resolved SR Ca depletions during global Ca release in confocal line-scan mode. After steady-state 1 Hz stimulation, the SR structure of Fluo-5N loaded cells was discernible (Fig 1A). JSR is visible as narrow transverse bands of high fluorescence at ~1.9 μm intervals and FSR appears as faint longitudinal patterns between JSR regions, with variable intensity among FSR regions.[9,11] Recordings measure fluorescence from intra-SR localized Fluo-5N without appreciable cytosolic signal contamination. JSR is readily distinguishable from the weaker FSR signal (see below).

Figure 1B shows a longitudinal line-scan image (1 Hz stimulation) of 15 JSR and intervening FSR regions. When signals are normalized to diastolic intensity at each location (F/F_0) the localization of individual JSR and FSR regions is no longer apparent during diastole (by definition) or during systole (Fig 1C). The latter indicates that $[Ca]_{SR}$ depletion occurs in FSR (similarly to JSR). $[Ca]_{SR}$ depletions are detectable even at single JSR or FSR sites (Fig 1D, left) and averaging fluorescence (F) of 9 JSR regions over 8 consecutive steady state twitches illustrate the 50% higher diastolic F at JSR vs. FSR (Fig 1D, middle), while normalized F/F_0 signals are superimposable (Fig 1D, right). JSR signals are taken from the 1 μm region centered on the intense diastolic JSR signal, while FSR signals are taken from the intervening 0.8-1 μm that we presume is centered at the M-line at the center of the sarcomere.

JSR and FSR depletion signals were analyzed in two different ways. First, a total of 1155 JSR and 753 FSR depletions from 17 cells were aligned at the beginning of the depletion, averaged and normalized (Fig 1E). The time-course of JSR and FSR $[Ca]_{SR}$ depletions were very similar, both in amplitude and kinetics. The time to 90% nadir was slightly longer in FSR vs. JSR (by 8 ms) suggesting a slight delay between JSR and FSR $[Ca]_{SR}$ depletion during release. Time constants of SR Ca refilling were very similar in JSR and FSR (159 and 140 ms respectively). The average depletion amplitude ($\Delta F/F_0$) was 0.30±0.02 for JSR and 0.31±0.03 for FSR, indicating no detectable $[Ca]_{SR}$ gradient at nadir. Based on previous calibrations,[11,14] this 30% decrease in Fluo-5N fluorescence corresponds to a 65% decreases in $[Ca]_{SR}$ from ~1300 to 460 μM.

Next, we analyzed the same SR Ca depletions by fitting individual JSR and FSR depletions with the product of a sigmoid decline and exponential recovery.[6,14,15] Kinetic fit parameters were averaged (Fig 1F-G). JSR and FSR, $[Ca]_{SR}$ depletion amplitudes were similar (0.31±0.03 and 0.32±0.03 $\Delta F/F_0$, respectively). Neither time to nadir of JSR and FSR depletions (101±13 and 88±12 ms, respectively; p = n.s.) nor the time constant of local $[Ca]_{SR}$ recovery was statistically different (153±24 and 140±26 ms, respectively). These results suggest that intra-SR Ca fluxes are relatively fast without detectable intra-SR [Ca] gradients at the resolution of our experiments. While there must be some $[Ca]_{SR}$ gradient between JSR release sites and FSR, such differences in kinetics and amplitude must be small. Thus Ca diffusion is relatively fast within a half-sarcomere, but this does not allow direct assessment of diffusion.

$[Ca]_{SR}$ gradients during spontaneous local SR Ca release events (blinks)

Global Ca transients and $[Ca]_{SR}$ scraps, where nearly all junctions release almost simultaneously is the opposite extreme for $[Ca]_{SR}$ depletion vs. an isolated spontaneous local SR Ca release (Ca spark or blink).[6] We analyzed spatio-temporal profiles of Ca blinks (measured simultaneously with Ca sparks). Figure 2 shows averaged Ca blinks and sparks during longitudinal (Fig 2A) line-scanning. At the time of local $[Ca]_{SR}$ blink nadir (~40 ms) the depletion is smaller in amplitude at longer longitudinal distance from the Z-line (50% smaller at a distance of 0.84 μm from Z-line; Fig 2C). At this same distance the time to nadir is also reached later in time (by ~11 ms). Thus, there are measureable spatiotemporal $[Ca]_{SR}$ gradients during local SR Ca release events.

Transverse line scans gave similar results (Fig 2B). However, the distance for half-maximal depletion was slightly smaller (0.76 vs. 0.84 μm) and the time to nadir occurred later (Fig 2D). Notably, this distance is similar to the transverse JSR spacing.[16]

This measureable spatiotemporal $[Ca]_{SR}$ depletion for Ca blinks, but not for Ca scraps seems dichotomous, but is not. This is because a single Ca blink can draw from an effectively infinite pool of SR Ca in 3-dimensions (and far away there is no $[Ca]_{SR}$ depletion). In contrast, when release occurs at each junction simultaneously, each half-sarcomere experiences the same $[Ca]_{SR}$ depletion, preventing net diffusion into the domain of one JSR from another. Indeed, each individual half-sarcomere (in 3-dimensions) would have reflective boundary conditions (no Ca flux across) and have similar extent of depletion. An alternative way to think about this is from the perspective of one mid-sarcomere FSR region. This region would only be slightly depleted during a blink at one neighboring Z-line, because that blink can draw Ca from regions in all 3 dimensions. For global SR Ca release, that FSR region may be the main reservoir for both adjacent longitudinal JSR regions, and consequently local $[Ca]_{SR}$ drops faster and more extensively.

Variations in Ca blink kinetics

We previously showed that Ca blink kinetics at individual sites vary greatly, but are highly reproducible at a given site.[6] This contrasted with the associated Ca sparks which were similar at different loci. Moreover, we reported a correlation between long duration Ca blinks and JSR regions which were highly connected to other SR regions, as assessed by FRAP of intra-SR Fluo-5N.[6] Here, we segregated individual longitudinal Ca blinks from Fig 2 into two groups: Fast blinks (recovery $\tau<200$ ms; Fig 3A) and slow blinks ($\tau\geq200$ ms, Fig 3B). Notably, the Ca spark amplitude and kinetics were almost the same for both groups (Fig 3, top middle). This suggests that the amount and kinetics of SR Ca release are roughly comparable. However, the blinks that refilled slowly tended to have slightly longer time to nadir and larger extent of local $[Ca]_{SR}$ depletion. Faster blinks, on the other hand, also exhibited a 28% wider spatial profile (FWHM of depletion was 2.3 vs. 1.8 μm; Fig 3, bottom), and the $[Ca]_{SR}$ depletion nadir at 0.8 μm away from the spark site was considerably closer to that seen at the spark center.

These differences are consistent with the fast blinks being from JSR sites that are better connected (via diffusion) to neighboring SR regions than the sites that exhibit slow blinks (JSR sites more diffusionally isolated). That is, SR Ca release at a well connected JSR site causes larger/faster depletion in neighboring SR regions, and recovers faster once SR Ca release terminates (faster τ). The slightly deeper nadir in the slow JSR sites may better approximate the critical $[Ca]_{SR}$ shut-off threshold, because slower replenishment allows better temporal separation of release and refilling phases.

Intra SR diffusion: Fluo-5N FRAP

To directly test intra-SR diffusion, we performed FRAP in cardiomyocytes permeabilized after Fluo-5N SR loading. The confocal line-scan mode for bleaching and FRAP allows high temporal resolution and restricts the bleached region to a width of ~1.5 μm. Therefore, this protocol allows measurement of intra-SR diffusion on a sarcomeric scale. Scan lines positioned longitudinally (parallel to myocyte long axis) or transversely (perpendicular to long axis at z-line) provides selective measurement of transverse or longitudinal diffusion, respectively.

Figure 4A shows laser intensity profile and Fluo-5N fluorescence from which FRAP kinetics were fit (sum of two exponentials). After the 450 ms bleach period, fluorescence decreased by 56±2 and 65±2% (n = 25 and 33; $p<0.05$) of the pre-bleach intensity for transverse and longitudinal bleach, respectively.

The slow FRAP component was very similar for longitudinal or transverse FRAP (Fig 4B), and constituted ~60% of the total fluorescence recovery (time constant of ~36 s). The fast FRAP component (~40% of total FRAP), was faster in the longitudinal vs. transverse (τ_{fast} = 1.56±0.2 vs. 2.24±0.2 s; $p<0.05$; n = 25 and 33 cells). Thus, intra-SR diffusion is faster longitudinally than transversely. Fluo-5N fluorescence recovered more fully after transverse vs. longitudinal bleach (74.8±2.4 vs. 54.4±1.9%; $P<0.05$, n = 25 and 33 cells). Incomplete recovery is probably due to an immobile fraction of Fluo-5N (protein-bound or mitochondrial trapping) but may also be due in part to loss of total fluorescent indicator during bleach. The slightly faster longitudinal vs. transverse diffusion of Fluo-5N probably reflects geometric SR constraints.

We also analyzed single junction FRAP to test for variability in connectivity of individual release units as recently proposed.[6,17] Indeed, the FRAP time constants varied >10-fold between individual junctions (fits for 10 JSR regions and mean are shown in Fig 4C). The τ_{fast} varied from 484 ms to 3.8 s (mean 1.57±0.91 s) and τ_{slow} varied from 10.2 s to 47.2 s (mean 21.1±3.5 s). These results are consistent with the notion that the connectivity of individual release units within the SR varies substantially. Junctions that showed very fast FRAP may be comparable with well connected junctions.[6]

Cytosolic diffusion: Calcein FRAP

To compare intra-SR with cytosolic diffusion, we used the same FRAP protocol in intact myocytes loaded with the cytosolic fluorophore calcein. Cytosolic FRAP was much faster than within the SR and the kinetics were not different between longitudinal vs. transverse bleach. Therefore only longitudinal photobleach is reported (τ_{Fast}=0.44±0.07 s; 48±7% of the total recovery and τ_{Slow}=7±1.5 s; $p<0.05$ *vs.* τ_{fast}). Total FRAP extent was also the same in both directions (59±4 and 61±0.2% after longitudinal and transverse photobleach; n= 6-9 cells). Fast (and slow) τ for cytosolic calcein FRAP was ~4-6 times faster than for Fluo-5N in the SR. The faster calcein FRAP is partly due to its smaller molecular weight vs. Fluo-5N (622 vs. 958), but this would only explain a 24% slower diffusion coefficient for Fluo-5N (Supplemental Table S1). Thus, intra-SR diffusion is slower than cytosolic by a factor of ~3-4.

Mathematical model of $[Ca]_{SR}$ changes during SR Ca release

Since these are the first detailed spatiotemporal profiles of dynamic $[Ca]_{SR}$ gradients measured in cardiac myocytes, we created a relatively simple computational model to gain quantitative mechanistic insights. Fig 5A shows the model geometry global SR Ca release (where all junctions fire). We model a single half-sarcomere, and assume that boundary conditions are everywhere reflective (no Ca flux across). For example, longitudinally

beyond the sarcomere center (M-line), a mirror image $[Ca]_{SR}$ profile occurs approaching the next JSR region. The same holds for sarcomeres above, below, left and right, as well as across the z-line. We use our detailed rabbit ventricular myocyte model[18] to set overall Ca fluxes (including the SR Ca release flux time-course which was initially fixed; see on-line supplement). Ca is released from JSR into the cleft, and diffuses along the longitudinal axis both inside and outside the SR (20 sequential compartments) and SR Ca-ATPase is uniformly spread along the non-junctional SR to allow refilling. We included Ca buffering by calsequestrin only in the two JSR compartments.

We simulated global and local Ca transients for different apparent Ca diffusion coefficients (D_{Ca}^{SR}; Fig 5C). Figure 5B shows that $D_{Ca}^{SR}=60 \quad \mu m^2 s^{-1}$ (as previously estimated[10]) produces global and local $[Ca]_{SR}$ signals that resembles those measured experimentally (Fig 1), where there is very little difference in depletion amplitude within the half-sarcomere (<5%) and a relatively short delay (<20 ms). Figure 5C shows the D_{Ca}^{SR} -dependence of the $\Delta[Ca]_{SR}$ spatial gradient and delay time to nadir between the JSR compartment and one at 1 μm (M-line; x=1 vs. 0 μm). To mimic limited optical resolution, we also averaged compartments within 500 nm of the JSR (JSR signal) and of the M-line (FSR signal). If D_{Ca}^{SR} were 10 times smaller (6 $\mu m^2 s^{-1}$),[11] the $\Delta[Ca]_{SR}$ gradient and the delay time would have been easily detectable in Fig 1.

For release from only one junction (Ca blink), we must allow Ca diffusion from neighboring sarcomeres, extending model geometry and boundary conditions (Fig 5D). For simplicity, we included 2 neighboring sarcomeres in each direction from the central releasing junction (20 nearest junctions; see Supplemental Fig II). Further extension adds computational complexity, but unaltered results. Using the same SR Ca release flux as in Fig 5A-C, substantially greater spatial gradients occur, even at half-sarcomere distance of ~1 μm (Fig 5E). Note that the JSR-FSR [Ca] gradient at nadir is strikingly different for the global vs. isolated release, over a broad range of D_{Ca}^{SR} (Fig 5F). Moreover, $D_{Ca}^{SR}=60 \quad \mu m^2 s^{-1}$ produces similar spatiotemporal features as seen in Ca blink experiments in Fig 2. However, for the same driving SR Ca release waveform, the blink $[Ca]_{SR}$ nadir is not as deep (even in JSR) as in a global $[Ca]_{SR}$ depletion. This is unlike experimental data where they are comparable. An obvious explanation is that the blink can refill from all directions (not true for a scrap) which for the same release flux, limits the extent of JSR depletion during a blink. If $[Ca]_{SR}$ decline controls the shut-off of release,[6,14] then release ought to continue until the threshold $[Ca]_{SR}$ is reached.

Figure 6 shows simulated Ca blinks where SR Ca release activates as in Fig 5, but where termination is due to an exponential shut-off starting when $[Ca]_{SR}$ reaches 0.46 mM (see Online Supplement). We also use diastolic $[Ca]_{SR}$=0.76 mM and average $[Ca]_{SR}$ within 200 nm of the JSR and 0.8 μm compartment, for direct comparison to blinks in Fig 2. Ca spark and blink kinetics roughly match experimental data for $D_{Ca}^{SR}=60 \quad \mu m^2 s^{-1}$ (Fig 6A, center). D_{Ca}^{SR} greatly influences the kinetics and $[Ca]_{SR}$ gradient (Fig 6A). The $[Ca]_{SR}$ at nadir and the delay in time to nadir over a range of distances from the SR junction (Fig 6E) can be compared to experimental data in Fig 2C-D.

Figure 6B shows direct measurement of JSR and FSR (top, from Fig 2), our model with $D_{Ca}^{SR}=60 \quad m^2 s^{-1}$ (middle) and a model by Swietach *et al.*[12] using a much lower D_{Ca}^{SR} (bottom). Note that the latter model does not capture the FSR Ca depletion measured experimentally.

If transverse and longitudinal D_{Ca}^{SR} is the same, the model predicts little anisotropy in $[Ca]_{SR}$ kinetics at 0.8 μm away, but if SR diffusion is faster longitudinally (based on Fluo-5N FRAP data) and we make apparent D_{Ca}^{SR} similarly anisotropic, the experimentally observed anisotropy is mimicked (Fig 6C vs. 2A-B). We can also simulate fast/connected vs. slow/isolated junctions by varying D_{Ca}^{SR} (Fig 6D). More sophisticated models are needed, but this simple model is useful to explore spatiotemporal $[Ca]_{SR}$ gradients.

DISCUSSION

Our main findings are: 1) during ECC, no appreciable $[Ca]_{SR}$ gradients occur between JSR and FSR, 2) diffusion within the SR is faster in the longitudinal than transverse direction (unlike cytosolic diffusion which is isotropic), 3) spatiotemporal $[Ca]_{SR}$ gradients are measureable during isolated Ca blinks, 4) intra-SR diffusion of Fluo-5N is 3-4 fold slower than a similar sized fluorophore in the cytosol, and 5) intra-SR Ca diffusion varies locally, dependent on local SR connectivity. These results have important implications for understanding the dynamics of SR Ca handling and $[Ca]_{SR}$ homogeneity, which may be critical for normal synchrony of myocyte and heart contraction and arrhythmogenesis.

$[Ca]_{SR}$ gradients between SR Ca release and uptake sites

Analyzing a large number of Ca scraps (spatially resolved $[Ca]_{SR}$ decline during global SR Ca release) JSR-FSR $[Ca]_{SR}$ gradients or delays were undetectable. Of course there must be some $[Ca]_{SR}$ gradient and delay between the site of release and sites distant from release, but at the level of an individual sarcomere this appears to be small (<5%), brief (<10 ms) and difficult to detect. This places explicit constraints on models of Ca diffusion and intra-SR buffering. Wu and Bers[10] showed that the lumen of the entire SR network and nuclear envelope are continuous. Upon activation of SR Ca release during ECC, nuclear envelope [Ca] was deleted only ~60% of that for sarcomeric SR, and nuclear envelope [Ca] kinetics were delayed with respect to $[Ca]_{SR}$ (time to nadir was 50 ms longer and recovery time constant was 70 ms longer). So, over longer distances transient intra-SR [Ca] gradients are readily detected. Other reports also suggested $[Ca]_{SR}$ gradients during local SR Ca release from individual junctions (Ca blinks),[6,9,19] where neighboring junctions do not release simultaneously (as in Ca scraps[11]).

These are the first spatiotemporally detailed measurements of $[Ca]_{SR}$ during Ca sparks/blinks. During local Ca blinks fractional $[Ca]_{SR}$ depletion falls to about half the JSR value at ~0.8 μm away (i.e. about mid-sarcomere), and $[Ca]_{SR}$ depletion is negligible at the next longitudinal JSR region 2 μm away. There is also temporal delay in blink time to nadir with increasing distance from JSR. This indicates that these gradients are technically measurable, supporting the conclusion that $[Ca]_{SR}$ gradients are small when all junctions release simultaneously. The average $[Ca]_{SR}$ nadir for both local Ca blinks and global Ca scraps during ECC are very similar ($\Delta F/F_0$ ~0.3, or $[Ca]_{SR}$ ~400 μM).

The similar $[Ca]_{SR}$ nadir for JSR depletion during both Ca blinks and global Ca release (scraps), is consistent with SR Ca release termination occurring at a particular JSR $[Ca]_{SR}$ threshold.[3,6] During a global Ca scrap, each junction may shut off at that same local $[Ca]_{SR}$, but at that point the FSR between these sites has also reached this same level. Notably when Ca scraps occur at every junction during ECC a given FSR region will be depleted by at least the two nearest JSR regions (plus those in parallel sarcomeres). Our measurements of Ca scraps and blinks place novel quantitative constraints for SR Ca handling during ECC.

These observations agree with Ca blinks being fundamental local release events that add to compose global Ca scrap signals (as Ca sparks are to Ca transients), and that most of the Ca

involved in a release event normally comes from the region within ~1 μm of the junction (yielding little spatial summation). The latter differs from Ca sparks, where extensive spatio-temporal summation of Ca sparks results in larger and slower $[Ca]_i$ transients (due to spatio-temporal overlap).[6] The adequacy of local SR Ca to support JSR release is aided by JSR Ca buffering by calsequestrin, and allows SR Ca release to suffice for contractile activation without emptying the SR. Our analysis also suggests that the SR Ca release waveform during a blink may be more prolonged (vs. scraps), because local JSR takes longer to decrease to the release termination threshold $[Ca]_{SR}$ when there is a larger diffusional reserve.

Intra-SR Ca Diffusion Coefficients

Wu and Bers[10] used direct $[Ca]_{SR}$ measurements with Fluo-5N to measure intra-SR Ca diffusion and an apparent diffusion coefficient (D_{Ca}^{SR}) of ~60 $\mu m^2 s^{-1}$ (~10 times slower than in solution), but substantially faster than cytosolic D'_{Ca} in muscle (which is reduced by Ca binding to fixed binding sites; ~14 $\mu m^2 s^{-1}$).[20] Swietach *et al.*[12] estimated a slower D_{Ca}^{SR} in cardiac myocytes (8-9 μm^2/cm), using an indirect approach (cytosolic [Ca] changes in response to local caffeine application). These are apparent diffusion coefficients, which include effects of local Ca buffering and path tortuosity. In the cytosol, fixed high affinity Ca binding sites (with slow off-rates) contribute greatly to slowing apparent cytosolic Ca diffusion. Inside the SR, most of the Ca binding sites (like calsequestrin) have low affinity and rapid off-rates, and would hinder diffusion less. On the other hand, the SR network, while highly interconnected, follows a tortuous path, such that path tortuosity might be a larger constraint on Ca diffusion inside the SR. Indeed, fluorophore diffusion inside the SR is 3-4 times slower than in cytosol, suggesting that about half of the 10-fold slowing of Ca diffusion in SR is due to pathway tortuosity, whereas the rest may be due to relatively fixed buffers inside SR.[12]

We cannot explain why Swietach *et al.*[12] estimated a much smaller D_{Ca}^{SR} than Wu & Bers[10] or that we find here. However, their explanation, that Wu & Bers did not account for SR Ca leak and declining $[Ca]_{SR}$ during measurements is unfounded because direct $[Ca]_{SR}$ measurements were shown (Fig 7C within [10]) which exclude that explanation. Moreover, the elegant model by Swietach *et al.*[12] (using indirect D_{Ca}^{SR} estimates) fails to recapitulate FSR depletion during Ca blinks that we measure experimentally (Fig 6B). The precise definition of D_{Ca}^{SR} in each paper also differs slightly.

Regardless of absolute D_{Ca}^{SR}, our direct $[Ca]_{SR}$ measurements during ECC indicate that intra-SR Ca diffusion is fast enough to nearly abolish potential $[Ca]_{SR}$ gradients between JSR and FSR within our spatiotemporal resolution. Fast intra-SR diffusion is further evident from the results of our FRAP experiments, showing that even the high molecular weight molecule Fluo-5N can diffuse rapidly within the SR network. Our prior work estimated intra-SR diffusion coefficients for Fluo-5N and Ca that differed only by the amount expected for their difference in molecular weight.[10] This is most consistent with a situation where the main diffusional limitation is tortuosity (which would be the same for both) rather than binding to fixed buffers (which ought to differ). Here, cytosolic calcein in the cytosol and Fluo-5N in the SR show that Fluo-5N diffusion inside SR is ~3-4 times slower than in cytosol. This may reflect largely differences in tortuosity, but other factors (e.g. binding) cannot be excluded.

Ca flux rate depends not only on D'_{Ca}, but also on the [Ca] gradient (ΔC) and cross-sectional area (A; $J_{Ca} = D'_{Ca} A (\Delta C/\Delta x)$, where x is longitudinal distance). Even for the same D'_{Ca} in

cytosol and SR, higher Δ[Ca] in SR than cytosol greatly enhance longitudinal SR Ca flux rate. For a 2-fold concentration gradient ΔC would be ~500 μM in SR vs. <0.5 μM in cytosol).

Consequences of relatively fast intra-SR Ca diffusion

Relatively fast intra-SR Ca diffusion has several functional consequences. First it creates homogenous SR Ca driving force for release during ECC (preventing regions with low $[Ca]_{SR}$). It may also limit spontaneous SR Ca release (preventing regions with high $[Ca]_{SR}$). Furthermore, there is no major temporal delay between $[Ca]_{SR}$ recovery in the JSR and FSR (as implicit in some earlier models). If Ca diffusion is faster in SR than cytosol it could limit Ca wave propagation. That is, if depletion at one junction reduces $[Ca]_{SR}$ at the next junction, it reduces the likelihood that elevated $[Ca]_i$ will activate the downstream release site (due to $[Ca]_{SR}$ effects on ryanodine receptor gating). A single Ca spark may not decrease $[Ca]_{SR}$ appreciably at the next longitudinal junction 2 μm away (Fig 2C), but this may not be so true transversally where distance between JSR regions is only ~0.8 μm[16,21] or after a wave is already initiated (i.e. where multiple depleting events from the wave direction could increase local JSR ahead of the wave).

Data regarding local SR Ca and wave propagation is indirect and controversial. Acute SERCA blockade was reported to either accelerate or slow Ca waves.[5,22] One could argue that blocking SERCA either keeps local cytosolic [Ca] higher in the wave front, thereby enhancing propagation (preventing reuptake along the way), or that Ca reuptake along the wave drives $[Ca]_{SR}$ up ahead of the wave such that blocking uptake slows propagation by limiting $[Ca]_{SR}$. SERCA activity could have both of these competing effects (explored theoretically[23,24]). Direct $[Ca]_{SR}$ measurements during waves would help to resolve this apparent dichotomy.

Intra-SR diffusion is slightly anisotropic and junctions vary in connectivity

For cytosolic diffusion FRAP was the same longitudinally and transversely (as in homogeneous cell-free systems). Thus cytosolic calcein diffusion is relatively isotropic, despite highly organized myocyte structures, which differ longitudinally and transversely. In contrast, intra-SR FRAP was faster in the longitudinal vs. transverse direction. This must mean that longitudinal SR connections (e.g. around or between T-tubules) create less of a diffusional barrier than the transverse connections (e.g. between sarcomeres in parallel). Ca blink characteristics also suggest a faster longitudinal vs. transverse intra-SR Ca diffusion. That is, $[Ca]_{SR}$ depletion 0.8 μm away is smaller for transverse vs. longitudinal Ca blinks (Fig 2A vs. B) and the delays in time to nadir are longer in the transverse direction (Fig 2D). The functional consequence is not obvious, but it could contribute to differential transverse wave susceptibility as discussed above). The smaller transverse depletion might also be due, in part, to a closer reservoir of the Ca buffer calsequestrin, because of the greater proximity to neighboring JSR regions in the transverse direction. This intra-SR anisotropy differs from cytosolic Ca diffusion which appears isotropic because Ca sparks are symmetric in longitudinal and transverse directions.[25] For wave propagation, a transverse junction would see higher cytosolic [Ca] (because it is closer than the nearest longitudinal junction), and $[Ca]_{SR}$ may be relatively maintained (because of weaker transverse SR diffusion). Both of these effects would enhance transverse vs. longitudinal wave propagation.

FRAP analysis revealed large variation in individual junctions even within the same cell. This is consistent with recent work[6,17] showing that some SR Ca release units are much better connected within the SR network than others. This may not matter during physiological ECC, because $[Ca]_{SR}$ gradients are tiny and refilling depends primarily on SR Ca-ATPase. However, during Ca sparks/waves filling is predominantly diffusion-

dependent,[6] and there could be hetero-geneous refilling with some regions reaching threshold for release before others. That could contribute to arrhythmogenic substrate. Despite differential predominance of SR Ca-ATPase vs. diffusion, both global Ca scraps and local Ca blinks have similar recovery τ (150-200 ms). This is probably because SR Ca-ATPase is much faster during the larger global Ca transient, and can compensate for the diffusional component present only during the blink. Both our experimental data and mathematical model provide novel understanding of spatiotemporal dynamics of $[Ca]_{SR}$, and place novel constraints on how we view $[Ca]_{SR}$.

Supplementary Material

Refer to Web version on PubMed Central for supplementary material.

Acknowledgments

Sources of Funding

NIH grants HL30077 (DMB), HL80101 (DMB, LAB) HL62231 (LAB) and HL71893 (TRS).

Non-standard Abbreviations and Acronyms

AM	acetoxymethylester
$[Ca]_{SR}$	intra-SR fee [Ca]
D	apparent diffusion coefficient
D_{Ca}^{SR}	D for Ca within the SR
ECC	excitation-contraction coupling
F	fluorescence
F_0	diastolic fluorescence
FRAP	fluorescence recovery after photobleach
FSR	free SR
FWHM	full width at half maximum
JSR	junctional SR
K_d	dissociation constant
RyR	ryanodine receptor
SERCA	sarcoplasmic/endoplasmic reticulum calcium-ATPase
SR	sarcoplasmic reticulum
τ	exponential time constant
T-tubule	transverse tubule

REFERENCES

1. Bers, DM. Excitation-Contraction Coupling and Cardiac Contractile Force. 2nd ed.. Kluwer Academic Press; Dordrecht, Netherlands: 2001. p. 427
2. Dibb KM, Graham HK, Venetucci LA, Eisner DA, Trafford AW. Analysis of cellular calcium fluxes in cardiac muscle to understand calcium homeostasis in the heart. Cell Calcium. 2007; 42:503–512. [PubMed: 17509680]

3. Bassani JWM, Yuan W, Bers DM. Fractional SR Ca release is altered by trigger Ca and SR Ca content in cardiac myocytes. Am. J. Physiol. 1995; 268:C1313–C1319. [PubMed: 7762626]
4. Satoh H, Blatter LA, Bers DM. Effects of $[Ca]_i$, Ca^{2+} load and rest on Ca^{2+} spark frequency in ventricular myocytes. Am. J. Physiol. 1997; 272:H657–668. [PubMed: 9124422]
5. Lukyanenko V, Subramanian S, Gyorke I, Wiesner TF, Gyorke S. The role of luminal Ca^{2+} in the generation of Ca^{2+} waves in rat ventricular myocytes. J Physiol. 1999; 518:173–186. [PubMed: 10373699]
6. Zima AV, Picht E, Bers DM, Blatter LA. Termination of cardiac Ca^{2+} sparks: role of intra-SR $[Ca^{2+}]$, release flux, and intra-SR Ca^{2+} diffusion. Circ.Res. 2008; 103:e105–e115. [PubMed: 18787194]
7. Ogata T, Yamasaki Y. High-resolution scanning electron microscopic studies on the three-dimensional structure of the transverse-axial tubular system, sarcoplasmic reticulum and intercalated disc of the rat myocardium. Anat Rec. 1990; 228:277–287. [PubMed: 2260783]
8. Yamasaki Y, Furuya Y, Araki K, Matsuura K, Kobayashi M, Ogata T. Ultra-high-resolution scanning electron microscopy of the sarcoplasmic reticulum of the rat atrial myocardial cells. Anat Rec. 1997; 248:70–75. [PubMed: 9143669]
9. Brochet DX, Yang D, Di Maio A, Lederer WJ, Franzini-Armstrong C, Cheng H. Ca^{2+} blinks: rapid nanoscopic store calcium signaling. Proc Natl Acad Sci U S A. 2005; 102:3099–3104. [PubMed: 15710901]
10. Wu X, Bers DM. Sarcoplasmic reticulum and nuclear envelope are one highly interconnected Ca^{2+} store throughout cardiac myocyte. Circ Res. 2006; 99:283–291. [PubMed: 16794184]
11. Shannon TR, Guo T, Bers DM. Ca^{2+} scraps: local depletions of free $[Ca^{2+}]$ in cardiac sarcoplasmic reticulum during contractions leave substantial Ca^{2+} reserve. Circ Res. 2003; 93:40–45. [PubMed: 12791706]
12. Swietach P, Spitzer KW, Vaughan-Jones RD. Ca^{2+}-mobility in the sarcoplasmic reticulum of ventricular myocytes is low. Biophys J. 2008; 95:1412–1427. [PubMed: 18390622]
13. Picht E, DeSantiago J, Blatter LA, Bers DM. Cardiac alternans do not rely on diastolic sarcoplasmic reticulum calcium content fluctuations. Circ Res. 2006; 99:740–748. [PubMed: 16946134]
14. Guo T, Ai X, Shannon TR, Pogwizd SM, Bers DM. Intra-sarcoplasmic reticulum free [Ca] and buffering in arrhythmogenic failing rabbit heart. Circ Res. 2007; 101:802–810. [PubMed: 17704210]
15. Kubalova Z, Terentyev D, Viatchenko-Karpinski S, Nishijima Y, Gyorke I, Terentyeva R, da Cunha DN, Sridhar A, Feldman DS, Hamlin RL, Carnes CA, Gyorke S. Abnormal intrastore calcium signaling in chronic heart failure. Proc Natl Acad Sci U S A. 2005; 102:14104–14109. [PubMed: 16172392]
16. Parker I, Zang WJ, Wier WG. Ca^{2+} sparks involving multiple Ca^{2+} release sites along Z-lines in rat heart cells. J Physiol. 1996; 497:31–38. [PubMed: 8951709]
17. Zima AV, Picht E, Bers DM, Blatter LA. Partial inhibition of sarcoplasmic reticulum ca release evokes long-lasting ca release events in ventricular myocytes: role of luminal ca in termination of ca release. Biophys.J. 2008; 94:1867–1879. [PubMed: 18024505]
18. Shannon TR, Wang F, Puglisi J, Weber C, Bers DM. A mathematical treatment of integrated Ca^{2+} dynamics within the ventricular myocyte. Biophys J. 2004; 87:3351–3371. [PubMed: 15347581]
19. Terentyev D, Kubalova Z, Valle G, Nori A, Vedamoorthyrao S, Terentyeva R, Viatchenko-Karpinski S, Bers DM, Williams SC, Volpe P, Gyorke S. Modulation of SR Ca Release by Luminal Ca and Calsequestrin in Cardiac Myocytes: Effects of CASQ2 Mutations Linked to Sudden Cardiac Death. Biophys J. 2008
20. Kushmerick MJ, Podolsky RJ. Ionic mobility in muscle cells. Science. 1969; 166:1297–1298. [PubMed: 5350329]
21. Chen-Izu Y, McCulle SL, Ward CW, Soeller C, Allen BM, Rabang C, Cannell MB, Balke CW, Izu LT. Three-dimensional distribution of ryanodine receptor clusters in cardiac myocytes. Biophys J. 2006; 91:1–13. [PubMed: 16603500]
22. Keller M, Kao JP, Egger M, Niggli E. Calcium waves driven by “sensitization” wave-fronts. Cardiovasc Res. 2007; 74:39–45. [PubMed: 17336953]

23. Ramay HR, Jafri MS, Lederer WJ, Sobie EA. Predicting local SR Ca^{2+} dynamics during Ca^{2+} wave propagation in ventricular myocytes. Biophys J. 2010; 98:2515–23. [PubMed: 20513395]

24. Thul R, Smith GD, Coombes S. A bidomain threshold model of propagating calcium waves. J Math Biol. 2008; 56:435–463. [PubMed: 17786446]

25. Bányász T, Chen-Izu Y, Balke CW, Izu LT. A new approach to the detection and statistical classification of Ca^{2+} sparks. Biophys J. 2007; 92:4458–4465. [PubMed: 17400702]

26. Shannon TR, Ginsburg KS, Bers DM. Potentiation of fractional SR Ca release by total and free intra-SR Ca concentration. Biophys. J. 2000; 78:334–343. [PubMed: 10620297]

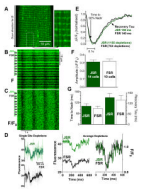

Figure 1. $[Ca]_{SR}$ depletion in junctional and free SR during global SR Ca release

A. 2-D confocal image of Fluo-5N loaded rabbit ventricular myocyte (with enlarged region). **B**. Line scan (direction indicated in A), where JSR and FSR regions are identified, **C**. fluorescence (F) from B normalized to local diastolic fluorescence (F/F_0). **D**. Raw fluorescence for single depletion at one JSR and one FSR region (thick trace is 5 point smooth; left) and F/F_0 for 9 FSR and JSR regions averaged for 8 Ca transients as F (middle) and F/F_0 (right). **E**. Averaged $[Ca]_{SR}$ depletions during whole cell Ca transients, normalized for number of indicated depletions. **F-G**. average parameters for fits of individual $[Ca]_{SR}$ depletions (number of cells indicated, for same total events as in E).

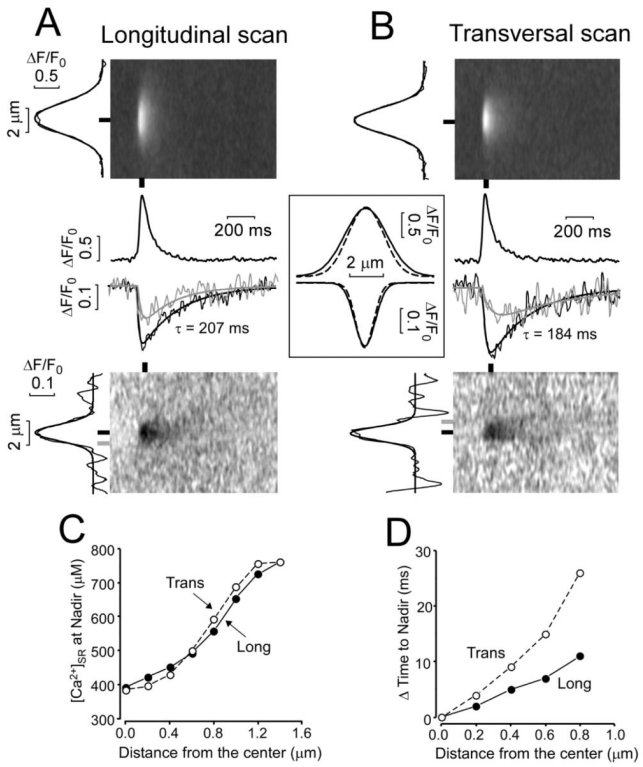

Fig 2. Ca sparks and Ca blinks in permeabilized ventricular myocytes

A. Averaged images of Ca sparks (***Top***) and Ca blinks (***Bottom***) recorded longitudinally, averaging 37 simultaneously measured events. Traces are for peak and nadir of each event (black lines and bars) and at 0.8 μm from the blink nadir (gray trace and bar). ***B.*** Same data analysis as in ***A*** for 27 averaged Ca sparks and blinks recorded transversally. Spatial profiles (width) of sparks and blinks are shown on left of images. Inset shows superimposed and amplitude normalized spatial profile at x=0 for longitudinal (solid) and transverse scans (broken). ***C.*** Relationships between $[Ca]_{SR}$ nadir and distance from center of SR Ca release. ***D.*** The relationships between delay to nadir (ΔTime) from that at x=0 (JSR) and distance from x=0.

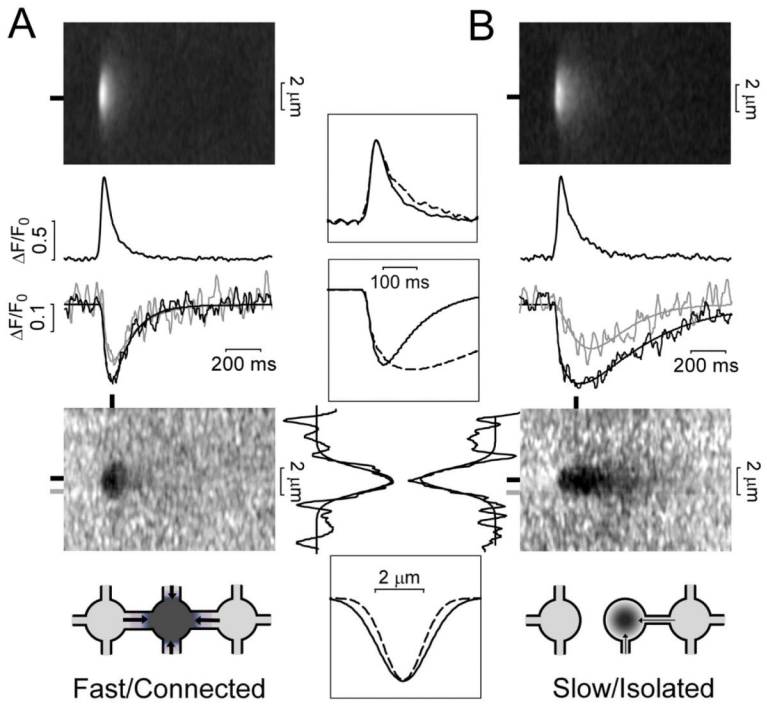

Fig 3. Fast vs. Slow Ca blinks in permeabilized ventricular myocytes

A. Averaged Ca spark (***Top***) and blink (***Bottom***) images (averaging 25 measured events recorded longitudinally with fast recovery kinetics, $\tau<200$ ms). Black traces are obtained at peak and nadir of each event (black bars). Gray trace shows $[Ca]_{SR}$ at a distance of 0.8 μm from blink center (gray bar). ***B.*** As in ***A*** for 12 Ca sparks/ blinks with slow blink recovery kinetic ($\tau\geq200$ ms). Insets show superimposed curves for fast/connected (solid) and slow/ isolated junctions (broken). Cartoons (bottom) shows how well-connected junctions may produce wider $[Ca]_{SR}$ depletion.

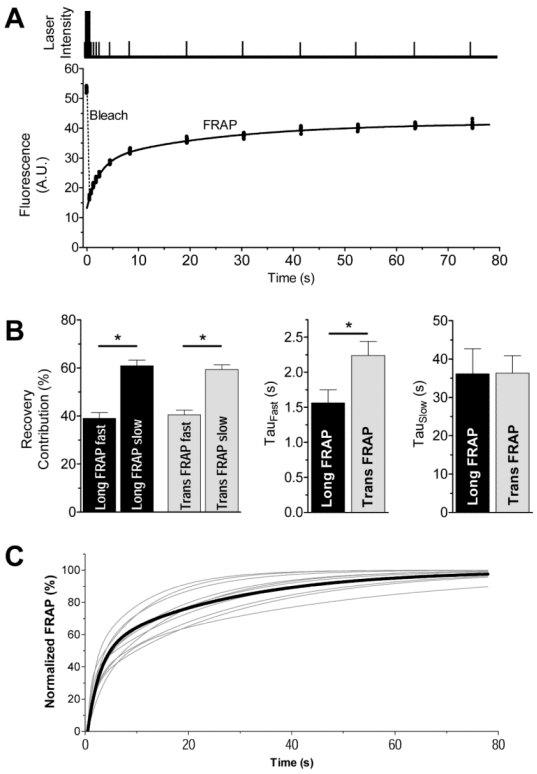

Fig 4. FRAP of SR-localized Fluo-5N in rabbit ventricular myocyte

A. Laser intensity (top, not to scale) showing bleach (tall) and measurement pulses (short) for a longitudinal scan and quantification on same time scale. **B**. FRAP bi-exponential fit parameters for scans in transverse (Long FRAP) and longitudinal directions (Trans FRAP). **C**. FRAP fits at ten individual JSR regions (thin lines) and mean longitudinal FRAP (thick line).

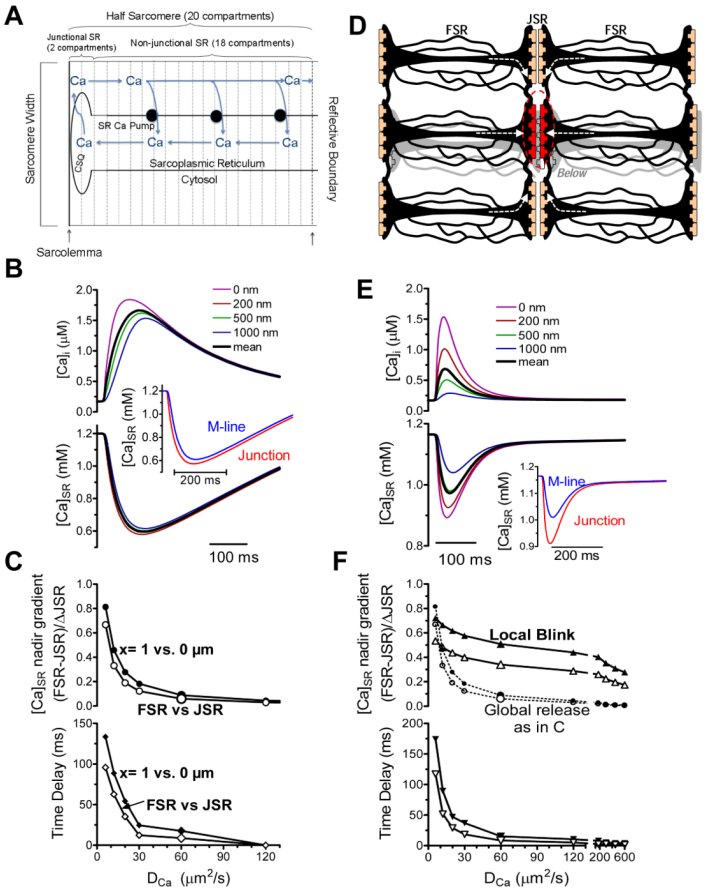

Fig 5. Mathematical model of $[Ca]_{SR}$ depletion during global & local SR Ca release

A. Compartments in ECC model. Ca Release takes place in a half-sarcomere with reflective boundaries. ***B.*** Cytosolic (top) and SR (bottom) free [Ca] at varying distances from SR junction, with model driven by SR Ca release waveform.[26] Inset shows mean data at junction and 1 μm away (±500 nm), simulating experimental data (Fig 1E). ***C.*** $[Ca]_{SR}$ gradient at nadir (top) and time delay to nadir at 1 μm vs. JSR over a range D_{Ca}^{SR} values. Filled symbols are for specific compartments, open symbols are compartment averages ±500 nm. ***D.*** Model geometry for release from a single red junction (see supplement Fig II). Arrows show how neighboring regions may supply Ca for release. ***E.*** Cytosolic and $[Ca]_{SR}$ profiles for release from a single junction in D. ***F.*** $[Ca]_{SR}$ gradient at nadir (top) and time delay to nadir at 1 μm relative to junction as in C. Top panel reproduces $[Ca]_{SR}$ gradients for ECC as in C (dotted).

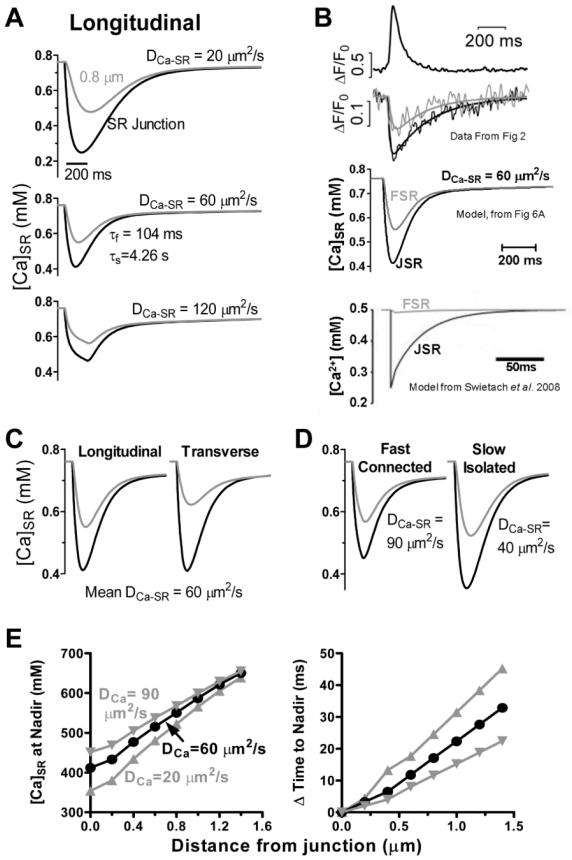

Fig 6. Modeling $[Ca]_{SR}$ depletion during Ca blinks

A. Ca release rate rises (τ=0.033 ms) to a plateau, until $[Ca]_{SR}$ falls to 0.46 mM. Release then terminates exponentially (τ=61 ms). Traces are average $[Ca]_{SR}$ within 200 nm of SR junction and 0.8 μm compartment. D_{Ca}^{SR} of 60 $\mu m^2 s^{-1}$ (middle) best matches experimental data (Fig 2A-B). ***B.*** Experimental measurements from Fig 2A, our model (from Fig 6A) and model by Swietach *et al.* (see text).[12] ***C.*** Longitudinal *vs*. transverse Ca blinks with D_{Ca}^{SR} adjusted based on FRAP differences in Fig 4D. ***D***. Fast/connected and slow/isolated junctions (as in Fig 3) are described by D_{Ca}^{SR} of 40 and 90 $\mu m^2 s^{-1}$, respectively. ***E.*** $[Ca]_{SR}$ nadir (left) and delay in the time to nadir (right) vs. distance from JSR (as in Fig 2C-D).